Optimal Fishery with Coastal Catch

Hannes Uecker* **Thorsten Upmann†**

September 29, 2017

Abstract

In many spatial resource models it is assumed that the agent is able to determine the harvesting activity over the complete spatial domain. However, agents frequently have only access to a resource at particular locations at which the moving biomass, such as fish or game, may be caught or hunted. In this paper, we analyse such an optimal control model with boundary harvesting. Using Pontryagin's Maximum Principle, we derive the associated canonical system, consisting of a forward–backward diffusion system with boundary controls, and numerically compute the canonical steady states and the optimal time dependent paths. We thus characterise the optimal control and the associated stock of the resource, and study the dependence of the optimal policies on the cost parameters. We begin with some simple one species models, and then extend the analysis to a predator–prey model of the Lotka–Volterra type, and show how the presence of two species enriches the results of our basic model. These models are rather generic, and structurally similar problems exist in other economic domains. Therefore, our methods are applicable to a large class of economic models with boundary controls.

Keywords: boundary control; bioeconomics; optimal harvesting; coastal fishing; infinite time horizon; predator–prey model; Lotka–Volterra

JEL Classifications: Q22, C61

Acknowledgements: We would like to thank the participants of the 16th Journées Louis-André Gérard-Varet, Aix-en-Provence, 2017; the Research Seminar on Environment, Resource and Climate Economics, MCC Berlin, 2017; the 6th International Workshop on Heterogeneous Dynamic Models of Economic and Population Systems, WU Vienna and, in particular, Vladimir Veliov and Charles Figuières for valuable comments and suggestions.

*Institut für Mathematik, Universität Oldenburg, 26111 Oldenburg, Germany, hannes.uecker@uol.de

†Bielefeld University, Faculty of Business Administration and Economics, Postfach 10 01 31, 33501 Bielefeld, Germany; CESifo, Munich, Germany, TUpmann@wiwi.uni-bielefeld.de

1 Introduction

Optimal control theory is an important tool to design optimal harvesting strategies in the management of natural resources. While the early work only considers the temporal dimension, see, *e. g.*, the familiar monographs of Conrad and Clark (1987), Conrad (2010) and Clark (2010), more recent work captures the spatial dimension as well, and in particular considers spatially distributed optimal harvesting for spatially distributed resources. In this paper, we take a different perspective and assume a spatially distributed resource for which harvesting can only be done at locations on the boundary of the habitat of the species. This constraint on the distribution of harvesting effort may either result from legal or physical restraints where the agent is either not allowed or not able (possibly due to economic reasons) to harvest inside the habitat. For instance, often a substantial part of fishing takes place either at the shore or is done by near shore artisanal fisheries; also, since fishing or hunting may be banned within protected areas, such as nature reserves, national parks, marine protected areas, game reserves etc., fishing and hunting frequently happens at the boundaries of those protected areas, aiming at the 'spillover' to the non protected areas (see, for example, Fogarty and Murawski, 2004, Kellner et al., 2007, and McCauley et al., 2016). To model harvesting behaviour in these circumstances, we consider an agent who is limited to boundary harvesting, and explore the agent's profit-maximising behaviour. In this way, our analysis complements spatial resource economics; and beyond this, it also represents a methodological contribution to economic theory by demonstrating how the theory of boundary control may help solve significant economic problems.

The early models in spatial resource economics feature discrete patches, where at each location of the resource the stock evolves according to an ordinary differential equation (ODE). Migration of the biomass is then modelled as entry and exit of the biomass from one location to the other. Notably, Sanchirico and Wilen (1999) set up a bioeconomic model with a finite number of patches with migration of the biomass and reallocation of effort between patches, and demonstrate how biological and economic features jointly determine the equilibrium distribution of the biomass and the harvesting effort over space and time.

However, in many cases the continuous process of migration is more adequately described by partial differential equations (PDEs) characterising the spread or diffusion of the resource within the domain.[1] Accordingly, a branch of spatial resource economics has developed which originates from theoretical biology and applied mathematics and makes use of PDEs to model the migration of biomass, such as fish or wildlife. For various models of this class, characterisations of optimal controls have been established so that control theory can now readily be applied when the state variables (stocks of resources) are governed by PDEs.[2] In particular, necessary conditions of the maximum principle for infinite horizon intertemporal optimization problems with diffusion have been derived by Brock and Xepapadeas (2008),

[1] A presentation of population models with diffusion can be found, for example, in Aniţa (2000, sec. 1.2), Okubo and Levin (2001), Murray (2003) and the references therein.

[2] Notable examples are Bai and Wang (2005) who are able to generalise the spatially homogeneous approach (see, *e. g.*, Fan and Wang, 1998; Clark, 2010), and Bressan et al. (2013) who demonstrate the existence of a constant profit-maximizing harvesting rate when total harvesting activity is bounded by a capacity constraint.

which in particular may lead to the emergence of spatial heterogeneity of the resource and (harvesting) effort concentration; see also Brock and Xepapadeas (2005); Xepapadeas (2010); Brock and Xepapadeas (2010); Uecker (2016); Ballestra (2016); Grass and Uecker (2017) for applications.

Similarly, for instance, Leung (1995) investigates spatially distributed profit-maximizing harvesting policies in a predator–prey model with Lotka–Volterra type of interaction and diffusion.[3] Further optimal control problems in a diffusive predator–prey setting are studied by Fister (1997, 2001), Fister and Lenhart (2006) and Chang and Wei (2012).[4] While Fister (1997) considers harvesting of both the prey and the predator population (on the full spatial domain), the economic agent in Fister (2001) is interested in harvesting the predator only and merely appreciates the existing stock of the prey. In the latter model the author introduces a boundary control which allows for controlling the migration of the populations across the boundary (*e. g.*, a fence, mesh size of a net, filter).[5]

Here we analyse a related class of diffusive optimal control problems, where the agent only has access to a resource at particular locations at which the moving biomass, such as fish, may be caught or harvested. We start with a simple one-species infinite-time-horizon optimal control problem for a fishery model with diffusion and boundary catch, and then extend it to a two-species predator–prey model. Due to boundary harvesting in our approach, the no-flux or Neumann boundary conditions of previous models need to be modified to take into account the take-out of fish precisely at the boundary, *i. e.*, at the coast; this gives a Robin boundary condition at the point of take out.

For the scalar model in a one dimensional space, the characteristics of the candidates for optimal steady states, *i. e.*, optimal steady harvesting rates at the boundary and corresponding distributions of fish in the domain, can be obtained from a phase plane analysis of the state equation. However, to study optimal time-dependent paths and to extend the analysis to predator–prey models or other generalizations, we need to resort to numerical methods. Thus, we use the Pontryagin maximum principle to derive the so called canonical systems, *i. e.*, the necessary first order optimality conditions, for both models. The associated stationary problems are systems of non-linear elliptic PDEs where the controls determine the boundary conditions, and in order to compute their solutions, *i. e.*, the so called canonical steady states, we use the continuation and bifurcation software `pde2path` (Uecker et al., 2014). In a second step, we identify the optimal steady states and compute their canonical paths that characterise the policies to reach the optimal steady state in a profit-maximising way.

The method can be generalized to more complex boundary control problems, and as an example we also consider a two-species reaction-diffusion system of Lotka–Volterra type.

[3]The standard predator–prey model with Lotka–Volterra type of interaction can be found, for example, in Clark (2010, Section 8.2). For a survey of single and multi-species population models with diffusion see Okubo and Levin (2001) and Murray (2003).

[4]The corresponding simpler case of only one species and one control is studied by Stojanovic (1991); Leung and Stojanovic (1993); He et al. (1994, 1995).

[5]Belyakov and Veliov (2014) also investigate an optimal harvesting problem with an age-structured population of fish (but without spatial dimension) and selective fishing where only fish of prescribed size is harvested; a similar problem is dealt with by Quaas et al. (2013).

It turns out that for both classes of models, *i. e.*, the scalar one and the interacting species model, a "moderate harvesting policy" is optimal. This is quite intuitive as excessive fishing leads to a drastic diminution of the stock and thus impairs the conditions for future yield; while a moderate fishing activity forgoes present profits, but saves some of the stock for later catch and growth. Thus, in both the one-species and the two-species case a balanced fishing path is optimal. We complement our analyses by computing the evolution of the respective shadow prices and their spatial distributions in order to enhance the understanding for our findings. While in the one-species case the shadow price of fish is falling the more remote the fish is from the shore, this result need not necessarily be true for the predator in the two-species case, even though the net market value of the predator species is positive. Finally, we scrutinise how our results depend on the cost of fishing effort. In the predator–prey model, the asymmetric interaction between both species carries forward to asymmetric cost effects: While an increase in the fishing cost of the prey results in an increase in both stocks, an increase in the fishing cost of the predator leads to a decrease in the stock of the prey. In particular, if fishing of the predator is relatively costly, the value of that species may become negative, even though its market price exceeds the harvesting cost. Beyond this, we show that our qualitative results are quite robust with respect to the specification of the growth function of the biomass; still, polar parameter specifications may seriously affect, though in an intuitive way, the qualitative features.

Beyond the specific insights into optimal boundary harvesting achieved here, our analysis also makes a methodological contribution: our approach may be applied to other economic problems with diffusion where the control variables are restricted to the boundary of the domain. Problems of this type prevail quite frequently in economics: notable examples are the control of the proliferation of an infectious disease (epidemic) as a public health protection policy; the control of the flow of information in problems of advertising, information management or crowd motion and herding; the launch of new products when demand depends on consumer (the diffusion of) experience etc. Thus, this paper may help advance the consideration of boundary control methods in resource economics as well as in other areas of economics.

The remainder of the paper is organised as follows. In Section 2 we set up our basic one-species fishery model with boundary catch, provide a phase plane analysis of the constraints for the stationary case and derive the canonical system. In Section 3 we describe our numerical method, and present our results for the one species model. Section 4 contains the results of the two-species model, and in Section 5 we conclude by discussing our results and indicating possible directions for future research.

2 A Basic Model

Consider a fishery problem where harvesting (fishing) can be done on the boundary of an area populated by some species of fish. For example, think of a fisherman catching fish from the shore. For ease of tractability, we consider a one-dimensional space represented by the interval $\Omega := (0, l)$. Fishing can be done at location $x = 0$, the position of the fisherman, only. Let $v = v(x, t)$ be the biomass of fish at location $x \in \Omega$ at time $t \in \mathcal{T} \equiv [0, \infty)$.

The catch depends on the available biomass of fish v and on the harvesting effort k of the fisherman. Following, for example, Conrad and Clark (1987, p. 67), we specify the catch (or harvest) as a standard Cobb–Douglas function,

$$h = h(v, k) = v^{\alpha} k^{1-\alpha} \tag{1}$$

with $0 < \alpha < 1$.[6]

The fisher is interested in maximizing the profit from his fishing activity. Let $p > 0$ denote the market price of one unit of fish, and $c > 0$ the (constant) per unit cost of harvesting effort. Since fish is a non-durable good, the catch is offered at the market immediately when it is realised. Thus, we model the instantaneous profit from harvesting as

$$J_c(v, k) = ph(v, k) - ck.$$

The total growth of the stock at a given location x is governed by net growth of the biomass and movement of fish. Possible growth functions (net of mortality) are

$$f(v) = f_{\text{lin}}(v) := \delta - \beta v \qquad \text{(linear growth)}, \tag{2a}$$
$$f(v) = f_{\log}(v) := v(\delta - \beta v) \qquad \text{(logistic growth)}, \tag{2b}$$
$$f(v) = f_{\text{bi}}(v) := -v(v - \beta)(v - 1) \qquad \text{(bistable growth)}. \tag{2c}$$

For $f = f_{\text{lin}}$ the ODE $\dot{v} = f(v)$ has the unique globally stable fixed point $v^* = \delta/\beta$. For $f = f_{\log}$ we again have the stable fixed point v^* and, in addition, the unstable fixed point $v = 0$. For our purposes both models are quite similar: in particular, for each set of parameters both have a unique *canonical steady state* (CSS) (which refers to steady states of the canonical system, see below), showing similar qualitative behaviour. The main difference, though, is that for f_{lin} we can compute these CSSs semi-analytically, see section 2.2.1, which we then also use to validate our numerics. For $f = f_{\text{bi}}$, f is initially convex and then concave, with $\beta > 0$ representing the minimum viable population; thus, the growth function exhibits *critical depensation* (see Conrad and Clark 1987, p. 63 and Da Lara and Doyen 2008, p. 18f). As a consequence, for suitable parameters $f = f_{\text{bi}}$ yields multiple CSSs, although only one is economically relevant.

The movement of fish is modelled as diffusion, *i. e.*, by a term proportional to Δv, where Δ denotes the Laplace operator with respect to x.[7] Thus, the biomass of fish evolves according to the following system of differential equations and boundary conditions (BC)

$$\partial_t v = -G_1(v) := D\Delta v + f(v) \quad \text{in } \Omega \times \mathcal{T}, \tag{3a}$$
$$D\partial_n v(0,t) + g(v(0,t), k(t)) = 0 \quad \text{in } \mathcal{T} \quad \text{(control-dependent flux at the left boundary)}, \tag{3b}$$
$$\partial_n v(l,t) = 0 \quad \text{in } \mathcal{T} \quad \text{(zero flux at the right boundary)}, \tag{3c}$$
$$v(x,0) = v_0(x) \quad \text{in } \Omega, \tag{3d}$$

[6] This production function is more general than the frequently used bi-linear one that presumes that the catch per unit of effort is directly proportional of the density of fish.

[7] Although we focus on the one dimensional case $\Omega = (0, l)$, where $\Delta v = \partial_x^2 v$, we use dimension-independent notation where suitable for the purpose of possible generalization. See also Aniţa (2000, sec. 1.2) and the references therein for a presentation of population models with diffusion.

where D is the diffusion coefficient, n denotes the exterior normal to the boundary $\partial\Omega$, and the normal derivative on the left-hand side of equations (3b) and (3c) is defined as $\partial_n v(x) = \nabla v(x) \cdot n(x)$, where ∇ denotes the nabla (or gradient) operator. Thus, in the one-dimensional case we have $\partial_n v = -\partial_x v$ at the left boundary $x = 0$, and $\partial_n v = \partial_x v$ at the right boundary $x = l$.

Equation (3a) describes the total change in biomass resulting from autonomous growth and diffusion. It states that the rate of change of the state variable, *i. e.*, the concentration (or the biomass) of the resource, at a given point in space, is determined by the biological growth function f and by the movement (or dispersion) of the stock described by the term $D\Delta v$. The latter reflects the standard assumption that the flux of the stock is supposed to be proportional to the gradient of the size of the stock, with the movement of the stock taking place from places of high towards those of low concentration. In the one-dimensional case considered here we may assume that $D = 1$,[8] but for conceptual clarity and generalizations we keep D, for the moment. The fact that harvesting takes place at the left boundary of Ω motivates equation (3b), which represents the flux boundary condition at the left. It captures the fact that there is a negative input at $x = 0$: the negative of the value of the spatial derivative of the stock at $x = 0$, *e. g.*, $g > 0$ amounts to less fish at $x = 0$ than at some $x > 0$ close to $x = 0$. Since this spatial differential is induced by the harvest h, we specify g as

$$g(v, k) = \gamma h(v, k), \tag{3e}$$

for some $\gamma > 0$. Hence, equation (3b) represents the idea that a larger harvest at $x = 0$, *i. e.*, a larger take out of fish at the left, increases the differential in stocks between $x = 0$ and its (right) neighbourhood $x > 0$. Correspondingly, equation (3c) captures the idea that there is no fishing at the right boundary, and it thus represents the zero-flux (or Neumann) boundary condition at the right.

In equation (3e), γ can be thought of as the inverse of the replacement flux of fish: when γ is high (low) a given amount of fishing leads to a large (small) differential in stocks near to the location of the fisher, and this differential is due to a slow (fast) replacement of fish due to diffusion. Thus, in a simple setting γ could be chosen proportional to $1/D$, but we keep it as an independent parameter, essentially to possibly model special conditions for the replacement fluxes at the boundary.

Finally, given the instantaneous profit J_c, the agent seeks to maximize the total discounted profits

$$V(v_0) = \max_{k \in C([0,\infty), \mathbb{R}^+)} J(v_0, k), \text{ where } J(v_0, k) := \int_0^\infty \mathrm{e}^{-\rho t} J_c(v(0, t), k(t))\, \mathrm{d}t. \tag{3f}$$

We thus have an optimal control (OC) problem with the partial differential equation (PDE) constraints (3a)–(3e) and the boundary control k.

[8]The diffusion coefficient D should be understood as relative to the size of the domain Ω, and thus by rescaling the domain we may set $D = 1$.

2.1 Phase plane analysis of the steady state constraint

To get an intuition for the constraints in (3), we first sketch a phase plane analysis of the constraint in the stationary case, *i. e.*, for

$$v'' + f(v) = 0, \tag{4}$$

where we set $D = 1$, and as a shorthand notation write $v' \equiv \partial_x v$ and $v'' \equiv \partial_x^2 v$. Equivalently we can write (4) as a spatial dynamics system

$$v_1' = v_2, \quad v_2' = -f(v_1), \tag{5}$$

which is a Hamiltonian system with conserved energy:

$$E(v, v') = \frac{1}{2}v'^2 + F(v), \quad \text{with} \quad F' = f, \tag{6}$$

because $\frac{\mathrm{d}}{\mathrm{d}x}E(v(x), v'(x)) = v'(x)(v''(x) + f(x)) = 0$, and hence the orbits are level lines of E. For the specifications of f given in (2), we obtain

$$F_{\mathrm{lin}}(v) = \delta v - \frac{\beta}{2}v^2, \quad F_{\log} = \frac{\delta}{2}v^2 - \frac{\beta}{3}v^3, \quad F_{\mathrm{bi}}(v) = -\frac{\beta}{2}v^2 + \frac{1+\beta}{3}v^3 - \frac{1}{4}v^4. \tag{7}$$

Clearly, for all three models, $(v_1, v_2) = (1, 0)$ is a saddle point of the energy. From the modelling we know that we should only be interested in orbits of (4) with $v(x) > 0$ for all $x \in (0, l)$, with $v'(l) = 0$, and with $v'(0) > 0$ because we want a positive take-out at $x = 0$. For f_{lin} and $f_{\log}$ it is then easy to see that the only relevant solutions of (4) are those which start at $x = 0$ with $v(0) > 0$ and $v'(0) > 0$, and for which $v'(x)$ decreases monotonously to 0 at $x = l$. See Figure 1(a,b) for illustration, which also shows that both models behave rather similarly in the pertinent region of the phase space, *i. e.*, north-west of the fixed point $(1, 0)$.

On the other hand, for $f = f_{\mathrm{bi}}$ we have, in addition to the saddle at $(1, 0)$, a minimum of E at $(\beta, 0)$, surrounded by periodic orbits. Via linearisation of (5) around $(\beta, 0)$, we obtain the minimum period, given by $P_{\min} = 2\pi/\operatorname{Im}(\lambda_1)$ where $\lambda_1 = \overline{\lambda_2}$ are the eigenvalues of the linearisation. For instance, for $\beta = 0.6$ this yields $P_{\min} \approx 12.83$, and hence for a sufficiently large values of l, we can find orbits which start with $v(0), v'(0) > 0$ and $v'(l) = 0$, and which make a loop around $(\beta, 0)$, *i. e.*, are non-monotonic. See Figure 1(c) for an illustration.

Now, the crucial question is: which of these steady states are optimal, *i. e.*, maximize J_c in $\mathcal{S}$? Moreover, we are interested in the solution of the intertemporal OC problem (3). Thus, we next derive the necessary first order optimality conditions, known as the canonical system (CS).

2.2 Derivation and discussion of the canonical system

The so called canonical system formalism, also known as Pontryagin's Maximum Principle,[9] yields first order necessary optimality conditions. For our case where the harvesting effort k

[9] See Pontryagin et al. (1962), Raymond and Zidani (1999), Aseev and Kryazhimskii (2007) and Grass et al. (2008).

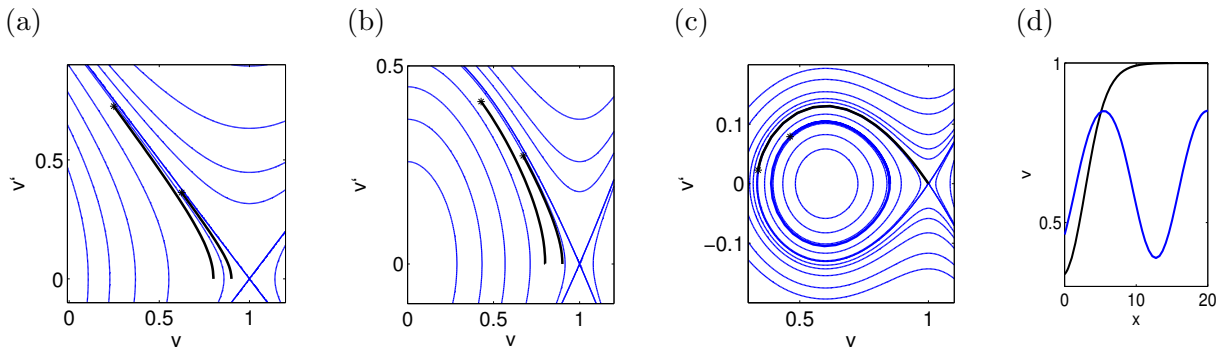

Figure 1: Phase plane analysis for (5), with (a) $f = f_{\text{lin}}$ and (b) $f = f_{\log}$, both with $\delta = \beta = 1$, and (c) $f = f_{\text{bi}}$ with $\beta = 0.6$. The blue lines are the level lines of the respective E, thus giving the phase portrait, while the black orbits (in (a,b)) are obtained from choosing $v(l)$ near 1, $v'(l) = 0$, *i. e.*, $(v_1, v_2)(l)$ near the fixed point $(1, 0)$, and integrating backward in time to $x = 0$, here for illustration with $l = 2$. The black dots thus indicate the "initial condition" at $x = 0$. In (c) we proceed similarly, but with $l = 20$ because of the minimal period $P_{\min} \approx 12.83$ of orbits around $(0.6, 0)$. We now find two families S_1 (monotonic, black example orbit) and S_2 (non-monotonic, blue example orbit) of orbits, see (d) for illustration of the x–dependence.

is a boundary control, we follow Tröltzsch (2010, Section 3.1) and consider the Lagrangian

$$L(v, \lambda, k) := \int_0^\infty \mathrm{e}^{-\rho t} \left\{ J_c - \int_\Omega \lambda(\partial_t v + G_1(v)) \,\mathrm{d}x \right\} \mathrm{d}t \tag{8}$$

where $\lambda : \Omega \times \mathcal{T} \to \mathbb{R}$ is the Lagrange multiplier for the PDE constraint, also called co-state variable, which may be interpreted as the shadow price of the biomass at location x at time t. Using integration by parts in x we have

$$\begin{aligned} \int_\Omega \lambda D \Delta v \,\mathrm{d}x &= -\int \langle \nabla\lambda, D\nabla v \rangle \,\mathrm{d}x + \int_{\partial\Omega} \lambda D \partial_n v \,\mathrm{d}s \\ &= \int (D\Delta\lambda) v \,\mathrm{d}x + \int_{\partial\Omega} \lambda(D\partial_n v) - (D\partial_n\lambda) v \,\mathrm{d}s, \end{aligned} \tag{9}$$

and integration by parts in t yields

$$-\int_0^\infty \mathrm{e}^{-\rho t} \int_\Omega \lambda \partial_t v \,\mathrm{d}x \,\mathrm{d}t = \int_\Omega \lambda(x,0) v(x,0) \,\mathrm{d}x + \int_0^\infty \mathrm{e}^{-\rho t} \int_\Omega (\partial_t \lambda) v \,\mathrm{d}x \,\mathrm{d}t, \tag{10}$$

where, since we may restrict our analysis to bounded state and co-state variables v and λ, we used the so-called transversality condition[10]

$$\lim_{t\to\infty} \mathrm{e}^{-\rho t} \int_\Omega \lambda(x,t) v(x,t) \,\mathrm{d}x = 0. \tag{11}$$

Evaluating the stock of fish by its shadow price λ, equation (11) specifies that the present value of the existing biomass living in Ω converges to zero as we consider the very distant future.

[10]See also, *e. g.*, Brock and Xepapadeas (2008, eq. (8)) for further discussion of this type of transversality conditions in PDE problems.

Next, using the BCs (3b) and (3c), *i. e.*, $D\partial_n v|_{x=0} = -g$ and $D\partial_n v|_{x=l} = 0$, we obtain

$$L(v,\lambda,k) = \int_\Omega v(x,0)\lambda(x,0)\,\mathrm{d}x + \int_0^\infty \mathrm{e}^{-\rho t}\Big\{ \big(J_c - \lambda g - (D\partial_n\lambda)v\big)\big|_{x=0} - (D\partial_n\lambda)v\big|_{x=l} \\ - \int_\Omega (\rho\lambda - \partial_t\lambda - \Delta\lambda)v - \lambda f(v)\,\mathrm{d}x\Big\}\,\mathrm{d}t. \tag{12}$$

The first variation of L with respect to v, applied to a test-function $\phi \in C^\infty(Q)$ with $\phi(\cdot,0) = 0$, yields

$$\partial_v L\phi = \int_0^\infty \mathrm{e}^{-\rho t}\Big\{ \big((\partial_v J_c - \lambda\partial_v g - D\partial_n\lambda)\phi\big)\big|_{x=0} - (D\partial_n\lambda)\phi\big|_{x=l} \\ - \int_\Omega (\rho\lambda - \partial_t\lambda - \Delta\lambda - \partial_v f(v))\phi\,\mathrm{d}x\Big\}\,\mathrm{d}t.$$

Therefore, by density of $C_0^\infty(Q)$ in $L^2(Q)$, $Q = \Omega\times\mathcal{T}$, and by density of $\partial_n C^\infty(\Omega)$ in $L^2(\partial\Omega)$, the condition $\partial_v L\phi = 0$ yields $\rho\lambda - \partial_t\lambda - \Delta\lambda - \partial_v f(v) = 0$ and the boundary conditions $D\partial_n\lambda - \partial_v J_c + \lambda\partial_v g = 0$ and $D\partial_n\lambda|_{x=l} = 0$. Thus, the CS is

$$\partial_t v = D\Delta v + f(v), \qquad v(x,0) = v_0(x), \tag{13a}$$
$$\partial_t\lambda = \rho\lambda - D\Delta\lambda - \partial_v f(v)\lambda, \tag{13b}$$
$$D\partial_n v + \gamma h = 0 \text{ at } x = 0, \qquad \partial_n v = 0 \text{ at } x = l, \tag{13c}$$
$$D\partial_n\lambda - (p - \gamma\lambda)\partial_v h = 0 \text{ at } x = 0, \qquad \partial_n\lambda = 0 \text{ at } x = l, \tag{13d}$$

where k is obtained from $k(t) = \operatorname{argmax}_k L(v(\cdot,t),\lambda(\cdot,t),k)$. In the absence of control constraints,[11] the condition $\partial_k L = 0$ yields

$$\begin{aligned} 0 &= \partial_k J_c - \gamma\lambda\partial_k h - v\partial_k(p - \gamma\lambda)\partial_v h \\ &= p\partial_k h - c - \lambda\gamma\partial_k h - v(p - \gamma\lambda)\partial_v\partial_k h = (p - \gamma\lambda)\partial_k h - (p - \gamma\lambda)\alpha\partial_k h - c, \end{aligned}$$

and thus

$$(p - \gamma\lambda)(1 - \alpha)\partial_k h = c \quad \Leftrightarrow \quad k = \left(\frac{(1-\alpha)^2(p - \gamma\lambda)}{c}\right)^{1/\alpha} v. \tag{13e}$$

System (13) summarizes the necessary first order optimality conditions for the optimal control problem (3). In particular, by equation (13e) the optimal effort is determined so that the value of the marginal product of effort equals its cost. This is because the term $\partial_k h = (1-\alpha)\,(v/k)^\alpha$ represents the marginal product of effort in harvesting, with $1-\alpha$ being the productivity of effort (or more precisely, the elasticity of the marginal product of effort in harvesting), and $p - \gamma\lambda$ represents the total value of one unit of biomass (fish) caught. In the first place, this value equals its market price p, however since each unit can only be caught once, future opportunities are impaired by any take out. More precisely, the extent to which a take out affects future catch depends on the influx or the replacement of fish at the coast (at the boundary), measured by γ. If γ is large, the replacement flux of fish is low,

[11] For instance, the natural constraint $k \geq 0$ can be checked *a posteriori* to be fulfilled.

so that the recovery of the stock takes time; on the contrary, if γ is low (and possibly zero in the limit) the replacement rate is high, so that the stock recovers quickly (and possibly instantaneously). Since λ equals the shadow price of fish, the term $\gamma\lambda$ represents the future reduction in the benefit of the catch due to today's take out of one unit of the biomass—and this value must be subtracted from the market price of fish.

We want to solve system (13) for k on the infinite time horizon $t \in [0, \infty)$, and thus at first might want to think of (13) as an initial value problem. However, equation (13a) provides initial data for only half the variables, while equation (13b) represents backward diffusion, implying that (13) is *not* an initial value problem. Instead, we proceed similar to Grass et al. (2008, Chapter 7), Grass and Uecker (2017) and Uecker (2016):[12] Letting $u \equiv (v, \lambda)$, we write (13) as

$$\partial_t u = -G(u), \quad u_1(x, 0) = v_0(x), \quad B(u) = 0, \tag{14}$$

where $B(u) = (B_1(u), B_2(u)) = 0$ encodes the boundary conditions at the left and right boundaries, respectively, and where we generally suppress the dependence on parameters.

Next we restrict condition (11) further to $\lim_{t\to\infty} u(t) = \hat{u}$, where $\hat{u}$ is a *canonical steady state* (CSS), *i. e.*, a steady state of the canonical system, and thus a solution of

$$G(u) = 0, \quad B(u) = 0. \tag{15}$$

In a first step we then numerically compute the CSSs. As (15) is (in general) a non-linear elliptic system, at a given set of parameters $(\rho, \alpha, p, c, \gamma, \beta)$ we may expect multiple CSSs, $\hat{u} = (\hat{v}, \hat{\lambda})$, with (generically) different values $J_c(\hat{v})$, or $J(\hat{v}) = \frac{1}{\rho} J_c(\hat{v})$, for different CSSs; and the question arises which of these CSSs maximizes J_c. In a second step, we want to find *optimal steady states* (OSSs), and their associated *optimal paths*. That is, given some initial state v_0, we want to compute *canonical paths* (CPs) connecting v_0 to some CSS $\hat{u}$, and then compare their respective values.

2.2.1 CSS for linear growth

A simple case where the CSS can be found semi-analytically is linear growth (2a):

$$f(v) = f_{\text{lin}}(v) = \delta - \beta v, \qquad \delta, \beta > 0, \tag{16}$$

with globally stable fixed point at $v^* = \delta/\beta$. The canonical system takes the form (with $D = 1$)

$$\partial_t v = v'' + \delta - \beta v, \qquad v(x, 0) = v_0(x), \tag{17a}$$

$$\partial_t \lambda = (\rho + \beta)\lambda - \lambda'', \tag{17b}$$

$$v'(0) = \gamma h, \quad v'(l) = 0, \qquad \lambda'(0) = -(p - \gamma\lambda)\partial_v h, \quad \lambda'(l) = 0. \tag{17c}$$

For the CSS, the general solutions of (17a,b) are

$$v(x) = \delta/\beta + a_1 \mathrm{e}^{\sqrt{\beta}x} + b_1 \mathrm{e}^{-\sqrt{\beta}x}, \quad \lambda(x) = a_2 \mathrm{e}^{rx} + b_2 \mathrm{e}^{-rx}, \qquad r = \sqrt{\rho + \beta}, \tag{18}$$

[12] See also Kunkel and von dem Hagen (2000) who, in sec. 4.2, consider optimal harvesting in a predator–prey ODE problem as an example.

where $\rho+\beta$ represents the compound "growth" rate consisting of the discount rate and the decay rate (or the reduction of the growth rate) of the natural stock.[13] It then remains to compute the constants a_1, a_2, b_1, b_2 from the BCs. From the Neumann BC at $x = l$ we get

$$b_1 = a_1 \mathrm{e}^{2\sqrt{\beta}l}, \quad b_2 = a_2 \mathrm{e}^{2rl}, \tag{19}$$

and thus end up with an algebraic system for a_1, a_2, namely

$$\sqrt{\beta} a_1 \big(\mathrm{e}^{2\sqrt{\beta}l} - 1\big) = \gamma k^{1-\alpha} v^{\alpha}, \qquad r a_2 \big(\mathrm{e}^{2rl-1}\big) = \alpha k^{1-\alpha} v^{\alpha-1}(p - \gamma\lambda), \tag{20}$$

together with $k = \left((1-\alpha)^2(p-\gamma\lambda)/c\right)^{1/\alpha}$, where it is understood that $\lambda = \lambda(0)$ and $v = v(0)$ are functions of a_1, a_2 via equations (18) and (19). Let

$$\Psi(x,a) := \frac{\mathrm{e}^{xa} + \mathrm{e}^{a(2l-x)}}{a(\mathrm{e}^{2la} - 1)}$$

gather all discount and (possibly negative) growth effects that happen at location x. Then, the solutions of (17) can be implicitly written as

$$v(x) = \delta/\beta - \gamma h(v(0), k)\Psi(x, \beta), \qquad \lambda(x) = (p - \gamma\lambda(0))\, \partial_v h\,(v(0), k)\, \Psi(x, r).$$

Thus, in the CSS, the spatial distribution of v and λ is determined by the single term that depends on the location: Ψ. Since δ/β equals v^*, the stock of the resource in the CSS equals its steady state value v^* minus some decrement, which depends on location x and on the decay rate β, but does not (directly) depend on the discount rate ρ. The shadow price of the resource equals the value of the marginal product of the stock, *i. e.*, the increase in the catch resulting from a small increase in the biomass (for a given effort), times the compound growth and discounting term Ψ at $r \equiv \sqrt{\rho+\beta}$. Since Ψ is decreasing in x, the stock is higher and the shadow price is lower at more distant locations. Both results mirror the fact that a take out of fish exclusively takes place at the boundary $x = 0$: due to the diffusion of fish, its removal at $x = 0$ is compensated by gradual replenishment, but since this process takes time the value of fish is lower at more distant locations.

Unfortunately, system (20) cannot be solved algebraically for $a_{1,2}$, *i. e.*, for $v(0), \lambda(0)$ and k, so that even for linear growth we have to rely on numerical methods eventually. However, (20) can immediately and conveniently solved in `Matlab` or similar systems. As an example, we choose the parameter specification

$$(\rho, \alpha, p, \gamma, \beta, \delta, l) = (0.02, 0.3, 1, 0.5, 0.01, 0.01, 20), \tag{21}$$

and let c vary between 0.1 and 2. For $c = 0.1, 1, 2$ we then obtain the unique solutions $(a_1, a_2) = (-0.167, 0.0014)$, $(a_1, a_2) = (-0.0077, 0.00022)$, and $(a_1, a_2) = (-0.0027, 0.00006)$, respectively. The associated solutions (18) are shown in Figure 2(a), and are identical to the direct numerical solution of (17) using `pde2path` (see section 3). Also, Figure 2(a) confirms our algebraic result that the stock of fish is increasing and its shadow price is decreasing as the distance to the fisherman, located at $x = 0$.

[13] Alternatively, $\rho+\beta$ may be viewed as the "growth adjusted discount rate".

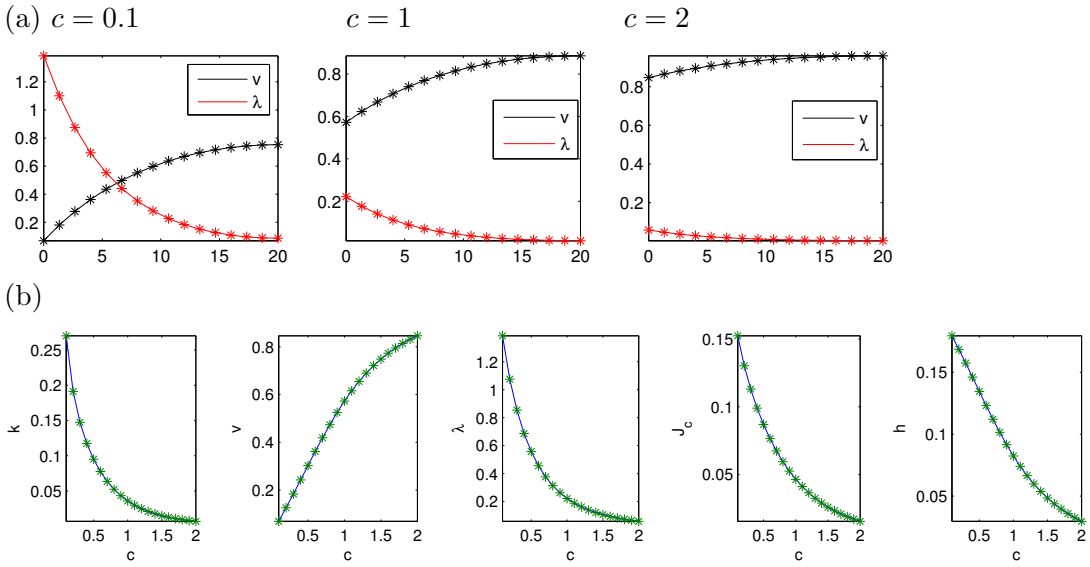

Figure 2: Some results for linear growth. In (a) we compare the solution (18) from (20) with parameters (21) (dots) with the direct numerical solution of (17) with `pde2path` (lines). Similarly, (b) compares the dependence of v, λ, k and J_c on c, computed via the two approaches.

2.2.2 Comparative statics

From equations (13e) and (20) we obtain $v = v(0)$, $\lambda = \lambda(0)$ and k as implicit functions of the cost parameter c; namely, using the shorthand $\Psi(a) = \Psi(0, a)$, we have

$$v = \frac{\delta}{\beta} - \gamma h\left(v,k\right)\Psi(\sqrt{\beta}),\ \ \lambda = \left(p-\gamma\lambda\right)\partial_v h\left(v,k\right)\Psi(r),\ \ c = \left(p-\gamma\lambda\right)\left(1-\alpha\right)\partial_k h\left(v,k\right). \tag{22}$$

Implicitly differentiating (1) and (22) with respect to c and solving for the desired derivatives yields

$$v'(c) = \frac{v\gamma k^{\alpha+1}\Psi\left(\sqrt{\beta}\right)\left(vk^\alpha + k\alpha\gamma v^\alpha\Psi(r)\right)}{(1-\alpha)\alpha(p-\gamma\lambda)\left(vk^\alpha + k\gamma v^\alpha\Psi(r)\right)\left(vk^\alpha + k\gamma v^\alpha\Psi\left(\sqrt{\beta}\right)\right)} > 0, \tag{23a}$$

$$k'(c) = -\frac{k^{\alpha+1}v^{-\alpha}\left(vk^\alpha + k\alpha\gamma v^\alpha\Psi(r)\right)\left(vk^\alpha + k\alpha\gamma v^\alpha\Psi\left(\sqrt{\beta}\right)\right)}{(1-\alpha)^2\alpha(p-\gamma\lambda)\left(vk^\alpha + k\gamma v^\alpha\Psi(r)\right)\left(vk^\alpha + k\gamma v^\alpha\Psi\left(\sqrt{\beta}\right)\right)} < 0, \tag{23b}$$

$$\lambda'(c) = -\frac{k^{\alpha+1}\Psi(r)}{(1-\alpha)\left(vk^\alpha + k\gamma v^\alpha\Psi(r)\right)} < 0, \tag{23c}$$

$$h'(c) = -\frac{v'(c)}{\gamma\Psi\left(\sqrt{\beta}\right)} < 0. \tag{23d}$$

An increase in the harvesting cost c renders harvesting effort more and more unattractive: with an increase in c, effort k is reduced implying a reduction in harvest h, and thus an increase in the stock v; in parallel, higher cost reduce the value of the stock λ. Correspondingly, the resulting profit falls with higher values of c. Figure 2(b) illustrates the dependence of these quantities on the effort cost c. Since the comparative effects (23) are unambiguous, it is clear that our numeric results depicted in Figure 2(b) are not due to our parameter specification but illustrate a general feature of our model.

3 Numerical method and results

3.1 Canonical steady states

For the special case of linear growth $f(v) = f_{\text{lin}}(v) = \delta - \beta v$, we have reduced the steady boundary value problem (17) to the (non-linear) algebraic problem (20). In general, such a reduction is not possible, and one has to resort to direct discretization of the canonical system. A standard method to get numerical insight into the (possibly non-unique) solutions u of a non-linear equation such as (15), and their dependence on parameters η, is as follows: one first seeks a solution $u_0(\eta_0)$ at some parameters values η_0. This first step is sometimes easy, for instance if there is a trivial solution $u = 0$, at least for some particular parameter values, and sometimes hard. In the latter case, one typically uses a guess $u^0(\eta_0)$, and then tries to improve this guess iteratively to a solution $u(\eta_0)$, for instance by the so called Newton method. Then, given a first solution $u(\eta_0)$, there are standard methods of so called numerical continuation (see Keller, 1977 and Doedel, 2007) to continue the solution in one or more parameters, *i. e.*, to find a nearby solution $u(\eta_0 + \delta)$, where δ is a small change of parameters. This can be repeated to obtain continuous branches of solutions. On these branches there may be bifurcation points, at which other branches of solutions bifurcate, and there are numerical methods to detect these bifurcations and compute the bifurcating branches.

`pde2path` is a `Matlab` package to do such a numerical continuation and bifurcation analysis for PDEs of type (14) (and also for more general PDEs) over one-, two- and three-dimensional domains. Moreover, it can also compute time-dependent canonical paths, and for instance Uecker (2016) applies this to a vegetation system with distributed controls, which leads to a four component reaction diffusion system with many different solution branches and associated bifurcations. The situation here turns out to be more simple though, and in particular we do not find bifurcations. Nevertheless, it is still useful to study the parameter dependence of the solutions, *i. e.*, the continuation of the solutions of system (14) (and of the generalization (34) below) in parameters.

3.1.1 Linear growth and logistic growth

In section 2.2.1 we already solved the problem for the CSS with $f = f_{\text{lin}}$ semi-analytically, and in Figure 2 we compared the solutions with those obtained from direct numerical solution of the associated system (14). The results match perfectly, also on varying other parameters than c, which illustrates the ease and robustness of using `pde2path` for problems of this kind.

For growth functions other than $f = f_{\text{lin}}$, we have to rely completely on numerical methods in order to be able to calculate CSSs. Still, the qualitative results for other specifications of f are quite similar to those of f_{lin}. In particular, for the case of $f = f_{\log}$, over economically reasonable parameter regimes, there is a unique CSS mapping $x \mapsto (v(x), \lambda(x))$ with $v' > 0$ and $\lambda' < 0$. Apparently, the reason for this similarity is the fact that $f(v) = v(\delta - \beta v)$ is positive in the relevant range $0 < v < v^* = \delta/\beta$ (see also our discussion of the phase plane in section 2.1). Accordingly, the dependence on parameters such as c is also qualitatively similar for logistic growth and linear growth.

3.1.2 Bistable growth

In our numerics of the CS (14) for $f = f_{\rm bi}$ we set $D = 1$ and $l = 20$, as we did in Figure 1(c,d), and hence *a priori* we know that for a CSS $\hat{u} = (\hat{v}, \hat{\lambda})$, $\hat{v}$ must belong to either the family $\mathcal{S}_1$ of monotonous steady states, or the family $\mathcal{S}_2$ of steady states with "loops". Thus, given parameter values of $(\rho, \alpha, p, c, \beta, \gamma)$, the steady-state of the canonical system (14), *i. e.*, the solution of (15), selects a discrete set of CSSs, some corresponding to the family $\mathcal{S}_1$ and some to $\mathcal{S}_2$. Additionally, we now fix

$$(\rho, \alpha, p, \beta, \gamma) = (0.03, 0.3, 1, 0.6, 0.5), \tag{24}$$

as a base parameter set for the canonical system (13); and as we did in Figure 2 for the case $f = f_{\rm lin}$, we take the costs of fishing effort $c \in (0, 2)$, which is the economically the most significant variable, as our primary continuation (or comparative statics) parameter.

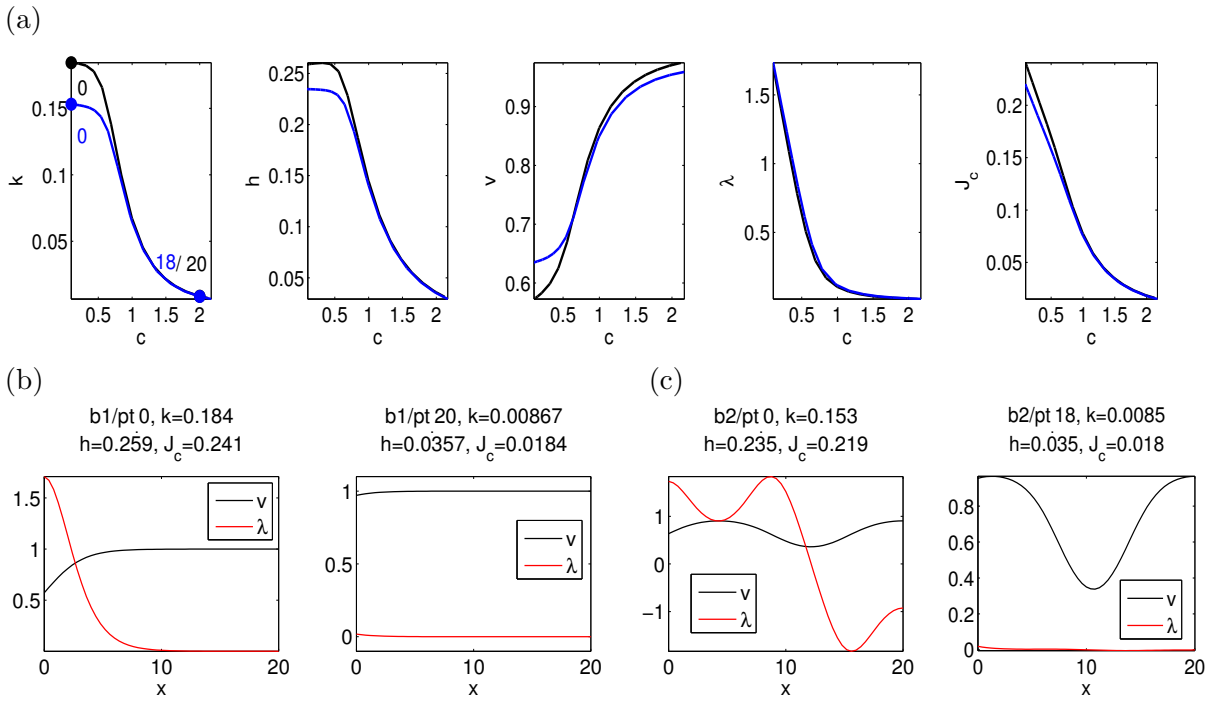

Figure 3: (a) Continuation diagrams in c for two branches of the CSSs of (13); the black branch (labelled `b1`) contains monotone solutions, while solutions on the blue branch (labelled `b2`) have 1.5 "loops" in v; v and λ in (a) at $x = 0$. See the example plots in (b) and (c), for $c = 0.1$ and $c = 2$.

Figure 3(a) shows two (obtained by different initial guesses for (v, λ)) branches of the CSSs as functions of the effort cost c. Along these branches, we display the harvesting effort k and the resulting harvest h, the biomass of fish v and the associated the co-state variable λ, as well as the implied instantaneous profit J_c. Figure 3(b) displays example plots of v and λ at the specific parameter values $c = 0.1$ and $c = 2$, together with the corresponding numbers for k, h and J_c.[14]

[14]The point labelling in the bifurcation diagram and the example plots follows the `pde2path` style `branch/pointnumber`.

Figure 3(a) confirms our findings of the linear model in section 2.2.1 (see Figure 2): an increase in the harvesting cost c leads to a reduction in the effort k and thus in the harvest h, and for that reason, to a fall of the profit J_c. Consequently, since an increase in c results in a fall of the value of the resource λ, and thus implies higher stock of the biomass v, a higher value of c represents an implicit protection of the resource. Focusing on the cases $c = 0.1$ and $c = 2$, Figure 3(b) depicts the spatial distribution of v and λ. If c is small (here $c = 0.1$), harvesting effort is high ($h = 0.259$); and since harvesting can only be done at the left boundary, the value of the resource is highest at $x = 0$ and is monotonously decreasing to zero for more remote populations. For high harvesting cost, harvesting becomes almost unprofitable implying that the value of the resource is close to zero even at the boundary $x = 0$. Since harvesting effort is low, the take out is marginal, and thus the stock is distributed almost equally on the domain $\Omega = (0, 20)$. The non-monotonic solutions associated to the blue branches in Figure 3(a) and with the solution plots in Figure 3(c) are sub-optimal, and economically implausible. This can clearly be seen by inspection of the co-state variable $\lambda(x)$, which becomes negative in parts of the domain.

3.2 The saddle point property, and canonical paths

In section 3.1 we identified the CSSs of system (3), *i. e.*, branches of solutions of the canonical system (15). Now, given an initial state v_0 we want to determine whether or not there exist *canonical paths* (CPs) connecting v_0 to some CSS $\hat{u}$. That is, we are interested in time dependent solutions $t \mapsto u(t)$ of (14) such that

$$u_1(x, 0) = v_0(x) \quad \text{and} \quad \lim_{t\to\infty} u(t) = \hat{u}. \tag{25}$$

This is a connecting orbits problem, not an initial value problem, as only the first component $u_1|_{t=0}{=}v_0$ is fixed, while $u_2|_{t=0}{=}\lambda|_{t=0}$ and hence the control $k(0)$ is free. Thus, different situations may arise:

1. There is a unique CP connecting v_0 to one CSS $\hat{u}$.
2. There is a unique CSS $\hat{u}$ which can be reached from v_0, but different CPs to do so.
3. Different CSSs $\hat{u}^{(1)}, \hat{u}^{(2)}, \ldots$ can be reached from v_0, and for each target there may be more than one CP;
4. There is no CSS $\hat{u}$ which can be reached from v_0.

If, given v_0, there is more than one CP, we can compare the respective values of J for those paths, and decide which one is optimal. Put differently, we can also consider a given CSS $\hat{u}$ and ask from which v_0 it can be reached by a suitably chosen CP. In particular, a CSS $\hat{u}$ that can be reached from all nearby v_0 and such that the associated CP maximizes $J(v_0, \cdot)$ is called a *locally stable optimal steady state* (OSS), while a CSS which can be reached from all v_0 that are admissible, *i. e.*, here all $v_0 \geq 0$ (pointwise), and such that the CPs maximize $J(v_0, \cdot)$, is called a *globally stable* OSS.

In general, all of the alternatives 1.–4. above can occur in a given system, and the domains of attraction of different locally stable OSSs are separated by so called Skiba manifolds; see, for example, Grass et al. (2008) for various ODE applications; and Grass and Uecker (2017) and Uecker (2016) for some PDE examples. However, here the situation turns out to be much more straightforward.

Since the computation of the CSS already required numerical methods, it is immediate that we have to rely on direct numerics when we want to compute canonical paths, irrespective of the specification of the growth function f. Numerically, we proceed as follows. Given the spatial discretization of $G(u) = 0$ with $2n$ degrees of freedom, *i. e.*, $u \in \mathbb{R}^{2n}$, (14) becomes a coupled system of $2n$ ODEs, which with a slight abuse of notation, we again write as

$$M\frac{\mathrm{d}}{\mathrm{d}t}u = -G(u), \quad u_1(x,0) = v_0(x), \quad B(u) = 0. \tag{26a}$$

Here $M \in \mathbb{R}^{2n\times 2n}$ is the mass matrix of the FEM (finite element method) approximation. We choose a truncation time T and approximate (25) by

$$u(T) \in E_s(\hat{u}) \text{ and } \|u(T) - \hat{u}\| \text{ small (in an appropriate norm)}, \tag{26b}$$

where $E_s(\hat{u})$ is the stable eigenspace of $\hat{u}$ for the linearisation $M\frac{\mathrm{d}}{\mathrm{d}t}\tilde{u} = -\partial_u G(\hat{u})\tilde{u}$ of (26). At $t = 0$ we already have the boundary conditions $v_{t=0} = v_0$ for the states. Then, in order to obtain a well-defined two point boundary value problem in time we need

$$\dim E_s(\hat{u}) = n. \tag{27}$$

Since the eigenvalues of the linearisation are always symmetric around $\rho/2$ (see Grass and Uecker, 2017, Appendix A) we always have $\dim E_s(\hat{u}) \leq n$. The number $d(\hat{u}) = n - \dim E_s(\hat{u})$ is called the *defect* of $\hat{u}$, a CSS $\hat{u}$ with $d(\hat{u}) > 0$ is called *defective*, and if $d(\hat{u}) = 0$, then $\hat{u}$ has the so called *saddle point property* (SPP). These are the only CSSs such that for general v_0 close to $\hat{u}$ we may expect a solution for the connecting orbits problem (26a), (26b). See Grass and Uecker (2017) for further comments on the significance of the SPP (27) on the discrete level, and its (mesh-independent) meaning for the canonical system as a PDE; and Uecker (2017a) for algorithmic details how to implement (26b), and how to find CPs connecting some v_0 to $\hat{u}$ by a continuation process in the initial states.

Linear growth and logistic growth. Using the `pde2path` numerics for the CS (17), we find that the unique CSS, computed in section 2.2.1, has the SPP, and that they are globally stable. An exemplary canonical path, starting at the globally stable fixed point $v \equiv 1$ of the unharvested system (17a) with homogeneous Neumann BC, and connecting to the CSS for $c = 0.1$ is shown in Figure 4(a,b); part (a) shows the behaviour of v under the optimal control, given by the red line in part (b), while the blue line shows the instantaneous profit. Of course, we could as well start with *any* v_0, but the idea of the simulation in Figure 4 essentially is that fishing starts at $t = 0$. The CPs then show exactly how to control the system to govern it to the OSS in an optimal way. The obtained strategy appears quite natural: one starts with a large harvest, which monotonically decreases to the value of the OSS harvest.[15] — Similar results are obtained for logistic growth.

[15]Note that while we have alternatively computed the CSS semi-analytically by reducing the steady canonical system to the algebraic system (20), it does not appear possible to reduce the time dependent canonical system to, e.g., a simple ODE on the boundary, and thus we use the PDE numerics to compute the canonical paths.

Bistable growth. For $f = f_{\rm bi}$, the CSSs of branch `b1` are the only CSSs with the SPP, and hence are globally stable OSSs, while all other CSSs $\hat{u}$, which make no economic sense anyway, have a defect $d(\hat{u}) > 0$. If we again compute the CP starting from the unharvested steady state $v \equiv 1$ to the OSS at the given parameters, then we obtain a picture similar to those for $f = f_{\rm lin}$ and $f = f_{\rm log}$, *i. e.*, one starts with a large harvest, which monotonically decreases to the value of the CSS harvest. In order to avoid replication, we start in Figure 4(c,d) from a depleted stock. For simplicity, we aim at the OSS at $c = 1$, and start with $v = v_0$ from the OSS at $c = 0.1$. While this is not a CSS at $c = 1$, it is a steady state for (3) with the fixed harvest $k \approx 0.184$, because (3) is a subsystem of the canonical system (13). Alternatively we can think of the associated canonical path as the optimal control in case that the cost c suddenly jumps from $c = 0.1$ to $c = 1$ at $t = 0$. The results are shown in Figure 4(c,d). As expected, the strategy is to first instantaneously decrease the effort from $k = 0.184$ to $k = 0.04$, thus allowing the stock to recover, and then monotonously increasing k to reach the new OSS.

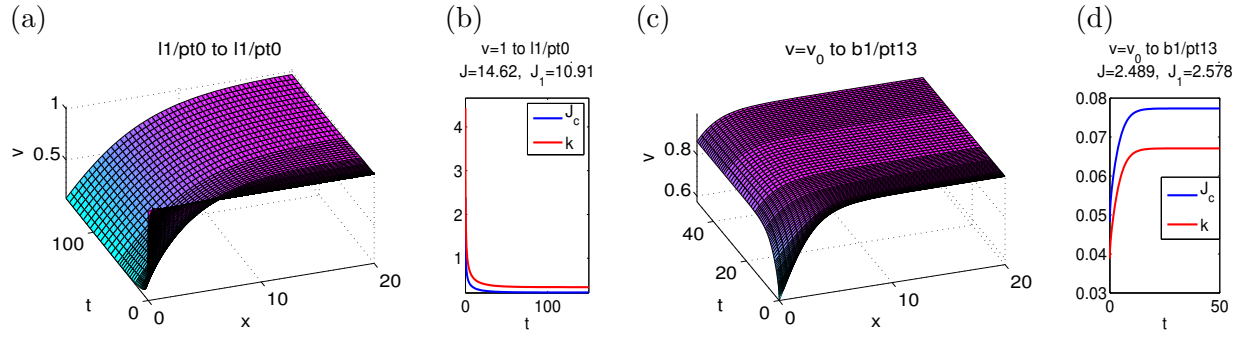

Figure 4: (a) The canonical path (v component) for linear growth, connecting $v = 1$ (globally stable fixed point of the unharvested system (17a) with homogeneous Neumann BC) as an initial state to the CSS at $c = 0.1$. (b) diagnostics: J and J_1 are the values of the CP and of the target CSS, respectively; and k, J_c are the control and the current value. (c,d) The analogues for $f = f_{\rm bi}$ at $c = 1$, where for variety here we start from a depleted stock, namely the v values which belong to the OSS for $c = 0.1$.

4 A predator–prey system

The scalar model of Section 2 can be greatly generalized. Here we consider a standard Lotka–Volterra system for two species: the prey (v_1) and the predator (v_2) in the form

$$\begin{aligned} \partial_t v_1 &= d_1 \Delta v_1 + (1 - \beta v_1 - v_2) v_1, \\ \partial_t v_2 &= d_2 \Delta v_2 + (v_1 - 1) v_2, \end{aligned} \tag{28}$$

with diffusion constants d_j, and self damping parameter of the prey $\beta > 0$. This system can more compactly be written as $\partial_t v = -G_1(v) = D\Delta v + f(v)$, with $D = \begin{pmatrix} d_1 & 0 \\ 0 & d_2 \end{pmatrix}$ and growth

function $f(v) = \begin{pmatrix}(1-\beta v_1 - v_2)v_1 \\ (v_1 - 1)v_2\end{pmatrix}$. Using the Liapunov function

$$\phi(v_1, v_2) = v_1 + v_2 - \ln v_1 - (1-\beta)\ln v_2 \tag{29}$$

it follows that

$$V^* = (v_1, v_2) = (1, 1-\beta) \tag{30}$$

is the unique steady state of the ODE system $\frac{\mathrm{d}}{\mathrm{d}t}v = f(v)$ in the first quadrant, and is globally stable. Similarly, using the functional

$$\Phi(t) = \int_\Omega \phi(v_1(t,x), v_2(t,x))\,\mathrm{d}x \tag{31}$$

it follows that for $d_{1,2}$ sufficiently large, V^* is the unique steady state of (28) with zero flux BC, and is globally stable, see, *e. g.*, Hastings (1978).

Analogous to (3) we consider a boundary fishing problem for the Lotka–Volterra system (28), and introduce J and controls via

$$J_c = \sum_{j=1}^{2} p_j h_j - c_j k_j, \quad h_j = h_j(v_j, k_j) = v_j^{\alpha_j} k_j^{1-\alpha_j}, \tag{32}$$

$$d_j \partial_n v_j = -g_j := -\gamma_j h_j \quad \text{as left BC.} \tag{33}$$

To apply Pontryagin's Maximum Principle we introduce the co-states $\lambda_{1,2}$ and the Lagrangian

$$L(v, \lambda, k) = \int_0^\infty \mathrm{e}^{-\rho t}\left\{J_c - \int_\Omega \langle \lambda, \partial_t v + G_1(v)\rangle\,\mathrm{d}x\right\}\mathrm{d}t,$$

where $\langle u, v\rangle = \sum_{i=1}^2 u_i v_i$ is the standard inner product in $\mathbb{R}^2$. Integration by parts in x and t now yields, similar to section 2.2,

$$\begin{aligned} L(v, \lambda, k) = &\int_\Omega \langle \lambda(0,\cdot), v(0,\cdot)\rangle\,\mathrm{d}x \\ &+ \int_0^\infty \mathrm{e}^{-\rho t}\Big\{[J_c - \langle \lambda, g\rangle - \langle D\partial_n\lambda, v\rangle]|_{x=0} - \langle D\partial_n\lambda, v\rangle\,|_{x=l} \\ &\quad - \int_\Omega \langle \rho\lambda - \partial_t\lambda - D\Delta\lambda, v\rangle - \langle \lambda, f(v)\rangle\,\mathrm{d}x\Big\}\mathrm{d}t. \end{aligned}$$

Then $\partial_v L = 0$ yields the evolution and the BCs of the co-states (combining with (28), to have it all together)

$$\left.\begin{aligned} &\partial_t v = D\Delta v + f(v), \\ &\partial_t \lambda = \rho\lambda - D\Delta\lambda - (\partial_v f(v))^T\lambda \end{aligned}\right\} \quad \text{in } \Omega = (0, l), \tag{34a}$$

$$\left.\begin{aligned} &D\partial_n v + g = 0, \\ &D\partial_n\lambda + \partial_v g(v)\lambda - \partial_v J_c = 0, \end{aligned}\right\} \quad \text{on the left boundary } x = 0, \tag{34b}$$

$$\left.\begin{aligned} &D\partial_n v = 0, \\ &D\partial_n\lambda = 0, \end{aligned}\right\} \quad \text{on the right boundary } x = l, \tag{34c}$$

and $\partial_k L = 0$ yields

$$k_j = \left(\frac{(1-\alpha_j)^2 (p_j - \gamma_j \lambda_j)}{c_j} \right)^{1/\alpha_j} v_j, \quad j = 1, 2. \tag{35}$$

As above, we first compute canonical steady states, *i. e.*, we start with the stationary version $G(u) = 0$, $u = (v, \lambda)$ of system (34), again on the domain $\Omega = (0, 20)$. We choose the base parameter set

$$(\beta, d_1, d_2, \gamma_1, \gamma_2, \rho, \alpha_1, \alpha_2, p_1, p_2) = (0.6, 1, 10, 0.1, 0.1, 0.03, 0.4, 0.4, 20, 10), \tag{36}$$

and consider the costs (c_1, c_2) as our continuation parameters, starting with $c_1 = c_2 = 0.1$. According to specification (36), we assume that the predator species moves faster than the prey, $d_2 = 10 > 1 = d_1$, and that the market price of the prey exceeds the price of the predator, $p_1 = 20 > 10 = p_2$, so that, disregarding the interaction of both species, the fisher is interested in catching the prey rather than the predator. Yet, in view of the interaction of the species, the fisher may consider catching the predator as well in order to "protect" the prey from being eaten by the former.

To find a CSS we use initial guesses of the form

$$v_1 = 1,\ v_2 = \delta(1-\beta),\ \lambda_1 = 50 + (1 - sx/l),\ \lambda_2 = 10 + (1 - sx/l), \tag{37}$$

with parameters $\delta \in (0, 1)$ and s close to 1, and some variations of (37). But if such an initial guess of this form yields convergence to a CSS, then (for the base parameters (36)) this convergence always leads to the same CSS. Note that a complete graphical phase plane analysis similar to section 2.1 is no longer possible, and thus it is not clear how many CSSs may exist for (34). However, given that for $d_{1,2}$ sufficiently large and zero flux BCs V^* is the unique steady state of the Lotka–Volterra system (28), it appears reasonable to expect that CSSs of system (34) are unique for the given parameter regime. (Note that we actually assumed rather large values for the diffusion parameters, $(d_1, d_2) = (1, 10)$, relative to the size of the domain.)

Figure 5 depicts the CSSs for the parameter specification (36), and their dependence on the cost parameters (c_1, c_2).[16] Parts (a) and (b) show relevant quantities at the left boundary as functions of c_1 and c_2, respectively, while part (c) shows the spatial shape of the CSSs for selected values of (c_1, c_2). As expected, an increase in c_i $(i = 1, 2)$ leads to a reduction in effort k_i and the associated harvest h_i, and thus brings forth a recovery of the stock v_i. In addition, an increase in c_i also imposes an indirect effect on v_{3-i} resulting from the interaction between both species. Consider an increase in the effort cost c_1. Clearly, there is no direct effect of c_1 on the fishing effort k_2 as the cost of this activity as well as the market price p_2 are unaffected. However, since an increase in c_1 results in less fishing effort k_1 and thus in a higher stock v_1, the living conditions of the predator species improve. Accordingly, the stock v_2 tends to increase, but since v_2 and k_2 are complements in the fishing technology, effort k_2 can be reduced with the catch h_2 still going up. Naturally, with higher cost c_1 the

[16] We can extend our analysis in any parameter of the model, but as explained above we confine ourselves to an analysis of the economically most immediate parameters c_1 and c_2.

(a) cont. in c_1, J, v, λ, k, h at $x = 0$

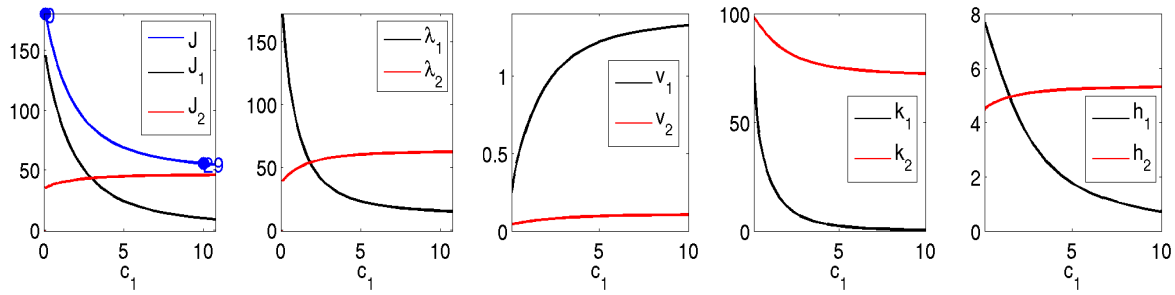

(b) cont. in c_2, J, v, λ, k, h at $x = 0$

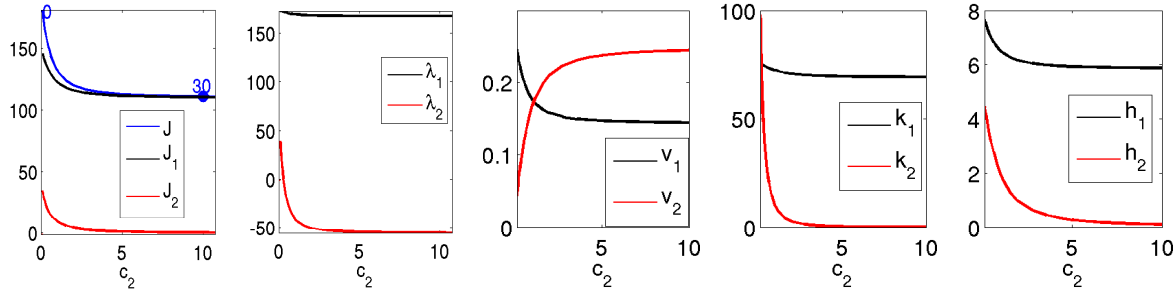

(c) CSS at $c = (0.1, 0.1)$, $c = (10, 0.1)$ and $c = (0.1, 10)$

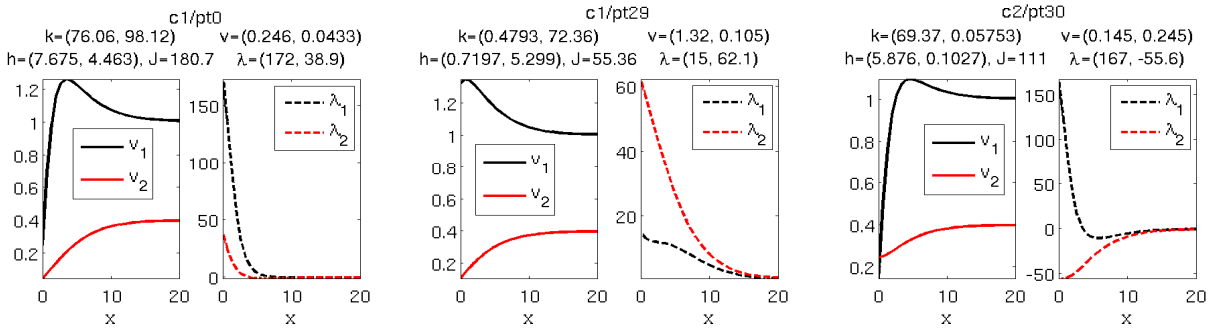

Figure 5: (a,b) continuation diagrams in c_1 (costs for prey fishing) and c_2 (costs for predator fishing); $J_j = p_j h_j - c_j k_j$, $J = J_1 + J_2$. For graphical reasons we restrict to $c_j \in [0.1, 10]$ (except for the plots of J) but all quantities continue as expected for $c_j \in [10, 20]$. (c) example CSS plots.

value of the the prey λ_1 falls, but the indirect effect, just explained, renders the value of the predator λ_2 to go up. The direct and the indirect effect of an increase in c_1 are also reflected in the profit terms. As expected, J_1 is a decreasing function of c_1, but the induced interaction effects between both species make J_2 to increase with c_1. Since the direct effect dominates, total profit J falls with higher cost.

Due to the biologically asymmetric situation of both species, the effect of an increase in c_2 has somewhat different indirect effects. In this case, higher effort cost c_2 lead to a reduction in effort k_2 and thus to increase in the stock v_2. But with an increase in the predator population the prey population becomes more threatened, rendering this population to decline; and for that reason the fishing activity k_1 is reduced. In this way, since the increase in the harvesting cost c_2 acts as a protection of the predator against being fished, the growth of that population exerts a negative effect on the prospects of fishing for the fisherman. Accordingly, with the population of the predator becoming sufficiently large, the value of a

unit of this species becomes negative. This explains why λ_2 is decreasing in c_2 and why it becomes (quickly) negative as the stock v_2 rises.

The qualitative structure of the spatial distribution of both species (and of the associated shadow prices) is quite robust with respect to changes in the costs c_1, c_2. Inspecting Figures 5(c1), (c2) and (c3), we infer that by catching the predator species the fisherman makes sure that its stock is kept low at the coast (left boundary) so as to safeguard the prey there. In fact, the stock of the prey reaches its maximum close to the coast, but harvesting at the coast causes the stock to decrease drastically there (unless c_1 is very high, see Figure 5(c2)). In any case, fish located close to the coast is more worthy than at more distant locations, where it is inaccessible for the fisherman, *i. e.*, λ_1 and λ_2 are both decreasing in x. There is one exception, though: when, as explained above, c_2 is sufficiently large, such that it is very expensive to catch the predator species, this stock may swell until it interferes with the prospects of the fisherman to catch the prey. In this case, the value of the predator is negative, $\lambda_2 < 0$, and because the damage caused by the predator species is the larger the closer it gets to the shore, λ_2 has its minimum directly at the shore.

(a) CP from V^* to the CSS at $(c_1, c_2) = (0.1, 0.1)$

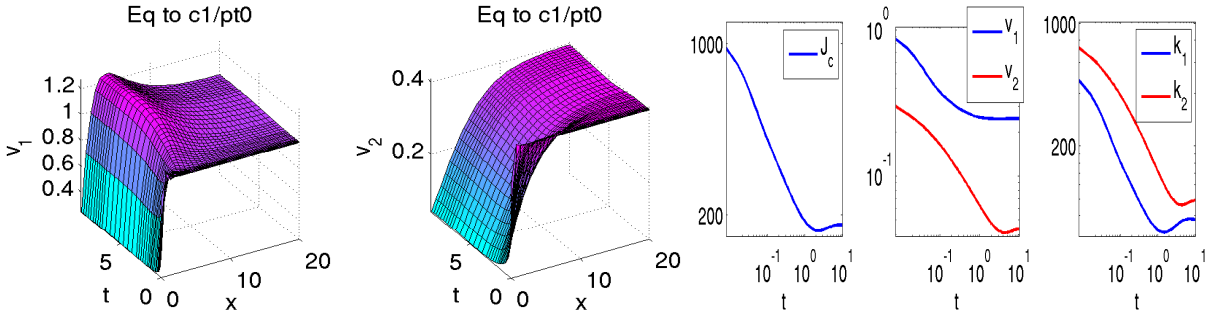

(b) CP from V^* to the CSS at $(c_1, c_2) = (10, 0.1)$

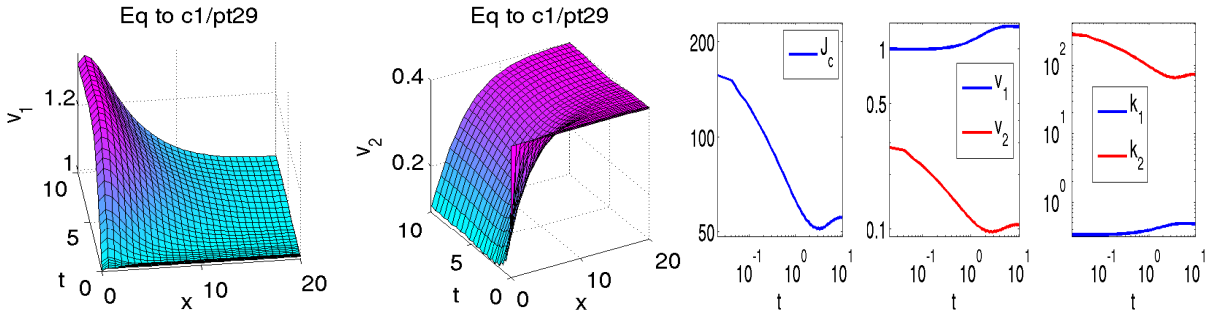

(c) CP from V^* to the CSS at $(c_1, c_2) = (0.1, 10)$

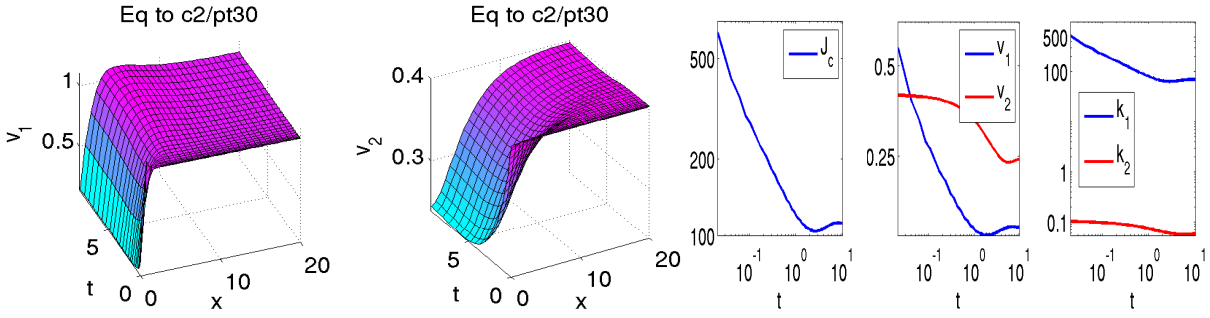

Figure 6: Canonical paths starting from the spatially homogeneous steady state V^* of (28).

In Figure 6 we illustrate the transition dynamics from the unique steady state (30) (with no fishing) to the CSS. Setting $(c_1, c_2) = (0.1, 0.1)$ in Figure 6(a) and $(c_1, c_2) = (20, 0.1)$ in Figure 6(b), these figures can directly be compared with Figure 5(c1) and Figure 5(c2), respectively. When the fishing cost of both species are low, $(c_1, c_2) = (0.1, 0.1)$, the transition to the CSS is accomplished by extensive fishing of both species at an initial phase, with fishing intensities decreasing from high towards low values. Thus, there is a some initial overfishing (because immediate profits are more desirable than those in the future due to the discounting), followed by a recovery phase during which the stocks of the CSS are reached from below, and during which the fisher increases the fishing intensity to that of the CSS.[17] Still, fishing effort is not monotonically decreasing, but exhibits non-monotonic behaviour. If fishing the prey is very costly, $(c_1, c_2) = (10, 0.1)$, the CSS is characterised by a low effort level k_1 and hence by a high stock of the prey, cf. Figure 5(c2) and 6(b). Similarly, along the CP leading to the CSS the main harvest is on the predator, with fishing effort being reduced over time, leading to the gradual increase of the prey at the left boundary—and eventually on the complete domain. However, some harvesting activity on the prey still takes place. Finally, for $(c_1, c_2) = (0.1, 10)$, the roles are basically reversed, subject to the indirect effects resulting from the implicit protection of the predator species by a high effort cost c_2, as explained above.

5 Discussion and extensions

To the best of our knowledge, in the context of economics, and in resource economics in particular, this is the first detailed numerical (and in section 2.2.1 semi-analytical) analysis of infinite time horizon optimal control problems with PDE constraints and a boundary control. We have set up one-species and two-species fishery models, computed the respective canonical steady states, singled out the optimal steady states and investigated the spatial distributions of the species and their respective values (shadow prices). Moreover, while previous studies in, *e. g.*, marine economics focus on those steady states, we also compute the canonical paths connecting some arbitrary initial state to the optimal steady state. These paths characterise the policies that achieve the optimal steady state in the most profitable way.

In all cases, the results appear natural and intuitive, and they are remarkably robust with respect to alternative specifications of the growth function—we considered linear, logistic and bistable growth functions—and with respect to changes in the effort cost of fishing. The optimal policy compromises between immediate and future yield, taking into account that a higher stock left in the lake may favour future growth of the resource. For the two-species Lotka–Volterra model, the asymmetric interaction between both species provides an additional incentive to catch the predator species in order to protect the prey for the purpose of own take out. This asymmetry between both species carries over to the spatial distribution of the biomass of both species and their respective shadow prices: while the shadow price of the prey is decreasing in the distance to the location of the fisherman (point of

[17] The initial transition is rather fast, and thus we use logarithmic scales in the time-series of the values at the left boundary.

take out), the shadow price of the predator may be higher at more distant locations. Also, we illustrated how the optimal policy depends on the relative effort cost of fishing either species. In particular, we showed that the shadow price of the predator may increase as the harvesting cost of the prey species go up.

Our approach can be extended to more complicated and realistic models. One obvious way would be to generalise the one-dimensional problem by, for instance, considering either spatially dependent coefficients (of the PDEs), or more intricate multi-species fishery models; in addition, we may take into account advection to model the transport of fish by flow. A second class of generalizations would be to extend the spatial domain to two (or even three) dimensions. The spatial domain could either take the form of depth dependence of fishing at a fixed position in a river with one horizontal dimension, of a lake, or of a marine reserve in the open sea. In all these cases we have a boundary control function defined on a given part of the boundary, rather than a scalar control. In the case of marine reserves, for instance, this modelling approach may yield quantitative results on optimal fishing of the spillover at the boundary.

Finally, our approach (either with one or multiple species) could be used to model competition between two or more agents (fishermen). Even in the basic model of a one-dimensional spatial space, the introduction of a second agent positioned, for example, at the other end of the one-dimensional lake would allow formulating an interesting non-cooperative dynamic harvesting game (*viz.* a differential game) in fishing activities.

References

Sebastian Aniţa. *Analysis and Control of Age-Dependent Population Dynamics*, volume 11 of *Mathematical Modelling: Theory and Applications*. Kluwer Academic Publishers, Dordrecht u. a., 2000.

S. M. Aseev and A. V. Kryazhimskii. The Pontryagin Maximum Principle and Optimal Economic Growth Problems. *Proceedings of the Steklov Institute of Mathematics*, 257(1): 1–255, 2007.

Ling Bai and Ke Wang. Gilpin-Ayala Model with Spatial Diffusion and its Optimal Harvesting Policy. *Applied Mathematics and Computation*, 171(1):531–546, 2005. doi: 10.1016/j.amc.2005.01.068.

Luca Vincenzo Ballestra. The spatial AK model and the Pontryagin maximum principle. *J. Math. Econom.*, 67:87–94, 2016.

Anton O. Belyakov and Vladimir M. Veliov. Constant Versus Periodic Fishing: Age Structured Optimal Control Approach. *Mathematical Modelling of Natural Phenomena*, 9(4): 20–37, 2014.

Alberto Bressan, Giuseppe Maria Coclite, and Wen Shen. A Multidimensional Optimal-Harvesting Problem with Measure-Valued Solutions. *SIAM Journal on Control and Optimization*, 51(2):1186–1202, 2013. doi: 10.1137/110853510.

William A. Brock and Anastasios Xepapadeas. Spatial Analysis in Descriptive Models of Renewable Resource Management. *Schweizerische Zeitschrift für Volkswirtschaft und Statistik*, 141(3):331–354, 2005.

William A. Brock and Anastasios Xepapadeas. Diffusion-induced Instability and Pattern Formation in Infinite Horizon Recursive Optimal Control. *Journal of Economic Dynamics and Control*, 32(9):2745–2787, 2008. doi: 10.1016/j.jedc.2007.08.005.

William A. Brock and Anastasios Xepapadeas. Pattern Formation, Spatial Externalities and Regulation in Coupled Economic-ecological Systems. *Journal of Environmental Economics and Management*, 59(2):149–164, 2010. doi: 10.1016/j.jeem.2009.07.003.

Xiaoyuan Chang and Junjie Wei. Hopf Bifurcation and Optimal Control in a Diffusive Predator-Prey System with Time Delay and Prey Harvesting. *Nonlinear Analysis: Modelling and Control*, 17(4):379–409, 2012.

Colin W. Clark. *Mathematical Bioeconomics*. John Wiley & Sons, New Jersey, 3rd edition, 2010. ISBN 978-0-470-37229-9.

Jon M. Conrad. *Resource Economics*. Cambridge University Press, Cambridge, 2nd edition, 2010. ISBN 978-0-521-69767-5.

Jon M. Conrad and Colin W. Clark. *Natural Resource Economics: Notes and Problems*. Cambridge University Press, Cambridge, 1987. ISBN 0-521-33188-9, 0-521-33769-0.

Michel Da Lara and Luc Doyen. *Sustainable Managment of Natural Resources: Mathematical Models and Methods*. Springer, 2008.

E. J. Doedel. Lecture Notes on Numerical Analysis of Nonlinear Equations. Krauskopf, Bernd (ed.) et al., Numerical continuation methods for dynamical systems. Path following and boundary value problems, 1–49, Springer., 2007.

Meng Fan and Ke Wang. Optimal Harvesting Policy for Single Population with Periodic Coefficients. *Mathematical Biosciences*, 152(2):165–177, 1998.

K. Renee Fister. Optimal Control of Harvesting in a Predator-Prey Parabolic System. *Houston Journal of Mathematics*, 23(2):341–355, 1997.

K. Renee Fister. Optimal Control of Harvesting Coupled with Boundary Control in a Predator-Prey System,. *Applicable Analysis*, 77(1–2):11–28, 2001.

K. Renee Fister and Suzanne Lenhart. Optimal Harvesting in an Age-Structured Predator-Prey Model. *Applied Mathematics and Optimization*, 54(1):1–15, 2006. doi: 10.1007/s00245-005-0847-9.

Michael J. Fogarty and Steven A. Murawski. Do Marine Protected Areas Really Work? *Oceanus Magazine*, 43(2):1–3, 2004.

Dieter Grass and Hannes Uecker. Optimal Management and Spatial Patterns in a Distributed Shallow Lake Model. *Electronic Journal of Differential Equations*, 1:1–21, 2017.

Dieter Grass, Jonathan P. Caulkins, Gustav Feichtinger, Gernot Tragler, and Doris A. Behrens. *Optimal Control of Nonlinear Processes: With Applications in Drugs, Corruption, and Terror*. Springer, 2008.

Alan Hastings. Global Stability in Lotka-Volterra Systems with Diffusion. *Journal of Mathematical Biology*, 6(2):163–168, 1978. ISSN 1432-1416. doi: 10.1007/BF02450786. URL `http://dx.doi.org/10.1007/BF02450786`.

Feiyue He, Anthony Leung, and Srdjan Stojanovic. Periodic Optimal-Control for Competing Parabolic Volterra–Lotka Type Systems. *Journal of Computational and Applied Mathematics*, 52(1-3):199–217, 1994.

Feiyue He, Anthony Leung, and Srdjan Stojanovic. Periodic Optimal-Control for Parabolic Volterra–Lotka Type Equations. *Mathematical Methods in the Applied Sciences*, 18(2): 127–146, 1995.

H. B. Keller. Numerical Solution of Bifurcation and Nonlinear Eigenvalue Problems. Application of bifurcation theory, Proc. adv. Semin., Madison/Wis. 1976, 359-384, 1977.

Julie B. Kellner, Irene Tetreault, Steven D. Gaines, and Roger M. Nisbet. Fishing the line near marine reserves in single and multispecies fisheries. *Ecological Applications*, 17(4): 1039–1054, 2007.

Peter Kunkel and Oscar von dem Hagen. Numerical Solution of Infinite–Horizon Optimal–Control Problems. *Computational Economics*, 16:189–205, 2000.

A. W. Leung. Optimal Harvesting-Coefficient Control of Steady-State Prey Predator Diffusive Volterra-Lotka Systems. *Applied Mathematics and Optimization*, 31(2):219–241, 1995. doi: 10.1007/BF01182789.

Anthony Leung and Srdjan Stojanovic. Optimal-Control for Elliptic Volterra–Lotka Type Equations. *Journal of Mathematical Analysis and Applications*, 173(2):603–619, 1993.

Douglas J. McCauley, Paul Woods, Brian Sullivan, Bjorn Bergman, Caroline Jablonicky, Aaron Roan, Michael Hirshfield, Kristina Boerder, and Boris Worm. Ending Hide and Seek at Sea. *Science*, 351(6278):1148–1150, 2016.

James D. Murray. *Mathematical Biology — II: Spatial Models and Biomedical Applications*, volume Mathematical Biology, Vol. 18 of *Interdisciplinary Applied Mathematics*. Springer, New York, 3rd edition, 2003. ISBN 0-387-95228-4.

Akira Okubo and Simon A. Levin. *Diffusion and Ecological Problems: Modern Perspectives*, volume Mathematical Biology, Vol. 14 of *Interdisciplinary Applied Mathematics*. Springer, New York, 2nd edition, 2001. ISBN 0-387-98676-6.

L. S. Pontryagin, V. G. Boltyanskii, R. V. Gamkrelidze, and E. F. Mishchenko. *The Mathematical Theory of Optimal Processes*. Wiley-Interscience, 1962.

Martin F. Quaas, Till Requate, Kirsten Ruckes, Anders Skonhoft, Niels Vestergaard, and Rudi Voss. Incentives for Optimal Management of Age-Structured Fish Populations. *Resource and Energy Economics*, 35(2):113–134, 2013.

J. P. Raymond and H. Zidani. Pontryagin's Principle for Time-Optimal Problems. *Journal of Optimization Theory and Applications*, 101(2):375–402, 1999. ISSN 0022-3239. doi: 10.1023/A:1021793611520.

James N. Sanchirico and James E. Wilen. Bioeconomics of Spatial Exploitation in a Patchy Environment. *Journal of Environmental Economics and Management*, 37(2):129–150, 1999.

Srdjan Stojanovic. Optimal Damping Control and Nonlinear Elliptic Systems. *SIAM Journal on Control and Optimization*, 29(3):594–608, 1991.

Fredi Tröltzsch. *Optimal Control of Partial Differential Equations*, volume 112 of *Graduate Studies in Mathematics*. American Mathematical Society, Providence, RI, 2010.

Hannes Uecker. Optimal Control and Spatial Patterns in a Semi-Arid Grazing System. *Natural Resource Modeling*, 29(2):229–258, 2016.

Hannes Uecker. Infinite time–horizon spatially distributed optimal control problems with pde2path – a tutorial, 2017a. Available at Uecker (2017b).

Hannes Uecker. `www.staff.uni-oldenburg.de/hannes.uecker/pde2path`, 2017b.

Hannes Uecker, Daniel Wetzel, and Jens D. M. Rademacher. pde2path — A Matlab Package for Continuation and Bifurcation in 2D Elliptic Systems. *Numerical Mathematics: Theory, Methods and Applications*, 7:58–106, 2014.

Anastasios Xepapadeas. The Spatial Dimension in Environmental and Resource Economics. *Environment and Development Economics*, 15(6):747–758, 2010. doi: 10.1017/S1355770X10000355.